Mechanism of Unassisted Ion Transport across Membrane Bilayers

Michael A. Wilson and Andrew Pohorille*

Contribution from the Department of Pharmaceutical Chemistry, University of California, San Francisco, California 94143, and NASA-Ames Research Center, Moffett Field, California 94035

Received December 1, 1995. Revised Manuscript Received April 26, 1996[⊗]

Abstract: To establish how charged species move from water to the nonpolar membrane interior and to determine the energetic and structural effects accompanying this process, we performed molecular dynamics simulations of the transport of Na^+ and Cl^- across a lipid bilayer located between two water lamellae. The total length of molecular dynamics trajectories generated for each ion was 10 ns. Our simulations demonstrate that permeation of ions into the membrane is accompanied by the formation of deep, asymmetric thinning defects in the bilayer, whereby polar lipid head groups and water penetrate the nonpolar membrane interior. Once the ion crosses the midplane of the bilayer the deformation "switches sides"; the initial defect slowly relaxes, and a defect forms in the outgoing side of the bilayer. As a result, the ion remains well solvated during the process; the total number of oxygen atoms from water and lipid head groups in the first solvation shell remains constant. A similar membrane deformation is formed when the ion is instantaneously inserted into the interior of the bilayer. The formation of defects considerably lowers the free energy barrier to transfer of the ion across the bilayer and, consequently, increases the permeabilities of the membrane to ions, compared to the rigid, planar structure, by approximately 14 orders of magnitude. Our results have implications for drug delivery using liposomes and peptide insertion into membranes.

I. Introduction

Ion transport across cell membranes is essential for a number of cellular functions. In cells, this process is aided by ion channels, carriers, and pumps which lower the free energy barrier associated with the transfer of ions from the polar aqueous environment to the nonpolar interior of the membrane. However, ions can permeate lipid bilayers even in the absence of special molecules to assist the transport. In the last 30 years, unassisted transport of charged species across lipid bilayers has received considerable attention[1−8] motivated by efforts to understand general issues of charge stabilization inside membranes[9] as well as a variety of practical problems including drug delivery, especially time-controlled drug release using liposomes as delivery vehicles,[10] incorporation of charged peptides into membranes,[11] microscale separation and recovery schemes,[7] and ion transport between two immiscible liquids, which is fundamental in electrochemistry.[12] Another area that motivates studies of ion permeation across membranes is the origin of cellular life.[13,14] At this early stage of evolution, the transport of ions must have proceeded without the complex molecules that aid this process in contemporary cells. Finally, understanding the mechanism of unassisted transport at a molecular level will offer valuable insight into mediated ion transport.[15]

The simplest treatment of this problem is based on a continuum dielectric model in which the water and the bilayer are represented as continuous dielectric media characterized by dielectric constants ϵ_w and ϵ_b, respectively, and separated by a sharp, flat boundary. The ion is modeled as a point charge located in the center of a cavity of radius a. The free energy, $\Delta A(TS)$, of transferring the ion from bulk water to the center of the bilayer of width d is expressed as[2]

$$\Delta A(TS) = \frac{q^2}{2a}\left[\frac{1}{\epsilon_b} - \frac{1}{\epsilon_w}\right] - \frac{q^2}{\epsilon_b d}\ln\left(\frac{2\epsilon_w}{\epsilon_w + \epsilon_b}\right) \qquad (1)$$

Assuming $\epsilon_w = 77.4$, $\epsilon_b = 1$, $d = 35$ Å, and $a = 1.68$ Å, which can be considered the effective ionic radius of Na^+,[16] we obtain $\Delta A(TS) = 91$ kcal/mol. For a more realistic estimate of $\epsilon_b =$

[⊗] Abstract published in *Advance ACS Abstracts,* June 15, 1996.

(1) (a) Bangham, A. D.; Standish, M. M.; Watkins, J. C. *J. Mol. Biol.* **1965**, *13*, 238−252. (b) Papahadjopoulos, D.; Bangham, A. D. *Biochim. Biophys. Acta* **1966**, *126*, 185−188. (c) Papahadjopoulos, D. *Biochim. Biophys. Acta* **1971**, *241*, 254−259. (d) Scarpa, A.; de Gier, J. *Biochim. Biophys. Acta* **1971**, *241*, 789−797. (e) Blok, M. C.; van der Neut-Kok, E. C. M.; van Deenen, L. L. M.; de Gier, J. *Biochim. Biophys. Acta* **1975**, *406*, 187−196. (f) Ogino, T.; Schulman, G. I.; Avison, M. J.; Gullans, S. R.; den Hollander, J. A. *Proc. Natl. Acad. Sci. U.S.A.* **1985**, *82*, 1099−1103. (g) El-Mashak, E. M.; Tsong, T. Y. *Biochemistry* **1985**, *24*, 2884−2888. (h) Georgallas, A.; MacArthur, J. D.; Ma, X.-P.; Nguyen, C. V.; Palmer, R. G.; Singer, M. A.; Tse, M. Y. *J. Chem. Phys.* **1987**, *86*, 7218−7229. (i) Cruzeiro-Hansson, L.; Mouritsen, O. G. *Biochim. Biophys. Acta* **1988**, *944*, 63−72.

(2) (a) Parsegian, V. A. *Nature* **1969**, *221*, 844−846. (b) Neumcke, B.; Läuger, P. *Biophys. J.* **1969**, *9*, 1160−1170.

(3) Hauser, H.; Oldani, D.; Philips, M. C. *Biochemistry* **1973**, *12*, 4507−4517.

(4) MacDonald, R. C. *Biochim. Biophys. Acta* **1976**, *448*, 193−198.

(5) Nozaki, Y.; Tanford, C. *Proc. Natl. Acad. Sci. U.S.A.* **1981**, *78*, 4324−4328.

(6) Deamer, D. W.; Bramhall, J. *Chem. Phys. Lipids* **1986**, *40*, 167−188.

(7) Hamilton, R. T.; Kaler, E. W. *J. Phys. Chem.* **1990**, *94*, 2560−2566.

(8) Deamer, D. W.; Volkov, A. G. In *Permeability and Stability of Lipid Bilayers*; Disalvo, E. A.; Simon, S. A., Eds.; CRC Press: Boca Raton, FL, 1995.

(9) Honig, B. H.; Hubbell, W. L.; Flewelling, R. F. *Ann. Rev. Biophys. Biophys. Chem.* **1986**, *15*, 163−193.

(10) Lasic, D. D. *Liposomes: from Physics to Applications*; Elsevier: Amsterdam, New York, 1993. See, also: *Science* **1994**, *265*, 316.

(11) (a) Seelig, J.; Nebel, S.; Ganz, P.; Bruns, C. *Biochemistry* **1993**, 9714−9721. (b) de Kroon, A. I.; de Gier, J.; de Kruijff, B. *Biochim. Biophys. Acta* **1991**, 111−124.

(12) Girault, H. H. J.; Schiffrin, D. J. In *Electroanalytical Chemistry*; Bard, A. J., Ed., Dekker: New York, 1989; p 1.

(13) Deamer, D. W.; Harang, E.; Bosco, G. In *Early Life on Earth. Nobel Symposium 84*; Bengtson, S., Ed.; Columbia U.P.: New York, 1993; p 107.

(14) Pohorille, A.; Wilson, M. A. *Origins of Life and Evololution of Biosphere* **1995**, *25*, 21−46.

(15) (a) Gennis, R. B. *Biomembranes: Molecular Structure and Function*; Springer-Verlag: New York, 1989. (b) Stein, W. D. *Channels, Carriers and Pumps*; Academic Press: San Diego, CA, 1990.

(16) Rashin, A. A.; Honig, B. *J. Phys. Chem.* **1985**, *89*, 5588−5593.

S0002-7863(95)04038-8 CCC: $12.00

2,[17] $\Delta A(TS)$ is reduced to 47 kcal/mol. This yields a membrane permeability of 10^{-29} cm s^{-1}, about 14−17 orders of magnitude lower than measured experimentally.[3,5,8] The width of the bilayer has only a small effect on these results: varying d from 20 to 80 Å changes $\Delta A(TS)$ only by 4 kcal/mol. For Cl^-, $\Delta A(TS)$ calculated from eq 1 for $\epsilon_b = 2$ is only 40 kcal/mol, due to a larger effective radius of this ion ($a = 1.94$ Å was used). This corresponds to a permeability coefficient of 10^{-24} cm s^{-1}. As has been noted previously,[4] the calculated ionic permeability depends on ionic size much more steeply than observed experimentally.

The simple continuum dielectric model is approximate even in bulk phases because other terms, not included in eq 1, also contribute to $\Delta A(TS)$. As has recently been pointed out,[18] this equation can be interpreted as an implementation of second-order perturbation theory for the electrostatic contributions to $\Delta A(TS)$. The zero-order term, the solvation free energy in the absence of charge, is not supplied by the dielectric model. The first order term, linear in the charge, is assumed to vanish. It would be true only if the water molecules around an uncharged cavity that accommodates the ion assumed random orientations. Finally, terms beyond the second order, which account for dielectric saturation, for example, are also neglected. Although a more complete treatment of the effects mentioned above would be beneficial for the description of charged and polar species in bulk media, it would not bring the calculated and measured membrane permeabilities to ions into agreement. Also, the large discrepancies between these two values cannot be simply explained by inaccuracies in choosing parameters for eq 1. In fact, with the choices of a adopted here, the model correctly predicts the enthalpies of Na^+ and Cl^- in aqueous solution.[16]

These discrepancies suggest that the model in which a "naked" ion is transferred across a sharp interface is inadequate and ignores some essential features of the transfer process that make important contributions to the free energy. Several alternative mechanisms of ion transport have been proposed that focus on deformations of the membrane and on reducing the loss of the hydration energy suffered by the ion inside the bilayer. For example, it has been postulated that ions are transferred across the bilayer with their first hydration shell intact[3] or that they move through transient defects[19,6] or pores[7] in the membrane rather than through an unperturbed nonpolar hydrocarbon interior.

Which mechanism provides the most faithful description of unassisted ion transport? What molecular-level changes in the water-membrane system accompany ion transfer, and how do they influence the energetics of this process? Since these questions are difficult to address experimentally, we have performed molecular dynamics computer simulations in which Na^+ or Cl^- was moved across the water-membrane system. These simulations have allowed us to elucidate the mechanism of ion permeation through membranes and to estimate the activation barriers and permeability coefficients for this process.

II. Method

The membrane constituent was glycerol 1-monooleate (GMO). Since this molecule is uncharged (and nonzwitterionic), this choice allowed us to avoid the computational complications associated with the presence of counterions in the system and to reduce the importance of long-range effects. Seventy-two GMO molecules were arranged in a bilayer between two lamellae of 1152 water molecules each. The total number of particles in the system was equal to 8857. Each lamella is approximately 25 Å wide. The x,y-dimensions (in the plane of the bilayer) were 37×37 Å^2. The simulation box was expanded in the z direction, perpendicular to the membrane, to 150 Å, so that during ion transport the system could relax freely in this direction. Thus, besides two water−membrane interfaces the system also contained two water liquid−vapor interfaces.

The water and GMO interaction potentials have been described previously.[20] Molecular dynamics simulations of the water−GMO system that employed these potentials yielded structural properties of the bilayer that agree very well with experimental data.[20] Here we only mention that water was represented by the TIP4P model.[21] The CH_n groups of the GMO hydrocarbon chains were treated as uncharged, united atoms with the total mass of the group located on the carbon atoms. All atoms in the glycerol head group were explicitly considered. Ion−water and ion−GMO interactions were represented as a sum of atom−atom Coulomb and Lennard-Jones contributions. The parameters for the latter terms were obtained by applying standard combination rules[22] using ϵ and σ for Na^+ and Cl^- from Jorgensen *et al.*[22] The ion−solvent interactions were truncated smoothly between 11.5 and 12 Å using a cubic spline switching function.[23] For water molecules, the oxygen atom was the cutoff center. For GMO molecules, a group based cutoff was used, as described in detail previously.[20] It would be desirable to employ an all-atom, polarizable model of the water-membrane system with a more rigorous treatment of long-range electrostatic effects. However, the simplifications employed here were necessary to obtain molecular dynamics trajectories sufficiently long to account for the reorganization of the system in response to progressive transfer of the ion.

To transfer each ion across the bilayer, a series of molecular dynamics trajectories was generated in which the ion was restricted to overlapping ranges ("windows") in the z-direction, perpendicular to the bilayer. The total length of these trajectories was approximately 10 ns for each ion. The equations of motion were integrated using the Verlet algorithm[24] with a time step of 5 fs. The temperature of the system was 300 K. Bond lengths and planar angles of both water and GMO were kept constant using the SHAKE algorithm.[25] The average ratio of the drift in the total energy to the total energy of the system during the course of simulation was 0.003 per 100 ps. To prevent the temperature from drifting away from its target value as a result of inaccurate integration of the equations of motion, velocities of particles were rescaled once the temperature deviated from 300 K by more than ±3 K. This occurred on average every 22 500 steps.

In each range, the change in the free energy of the ion along the z-direction, $\Delta A(z)$, could be calculated from the probability, $P(z)$, of finding the ion at position z[26]

$$\Delta A(z) = -kT \ln P(z) \qquad (2)$$

where k is the Boltzmann constant and T is the temperature of

(17) (a) Fettiplace, R.; Andrew, D. M.; Haydon, D. A. *J. Membr. Biol.* **1971**, *5*, 277−296. (b) Ohki, S. *J. Theor. Biol.* **1968**, *19*, 97−115. (c) Dilger, J. P.; Fisher, L. R.; Haydon, D. A. *Chem. Phys. Lipids* **1982**, *30*, 159−176.

(18) Pratt, L. R.; Hummer, G.; Garcia, A. E. *Biophys. Chem.* **1994**, *51*, 147−165.

(19) Nagle, J. F.; Scott, H. L. *Biochim. Biophys. Acta* **1978**, *513*, 236−243.

(20) Wilson, M. A.; Pohorille, A. *J. Am. Chem. Soc.* **1994**, *116*, 1490−1501.

(21) Jorgensen, W. L.; Chandrasekhar, J.; Madura, J. D.; Impey, R. W.; Klein, M. L. *J. Chem. Phys.* **1983**, *79*, 926−935.

(22) Jorgensen, W. L.; Madura, J. D.; Swenson, C. J. *J. Am. Chem. Soc.* **1984**, *106*, 6638−6646.

(23) Andrea, T. A.; Swope, W. C.; Andersen, H. C. *J. Chem. Phys.* **1983**, *79*, 4576−4584.

(24) Verlet, L. *Phys. Rev.* **1967**, *159*, 98−103.

(25) Cicotti, G.; Ryckaert, J. P. *Comput. Phys. Rep.* **1986**, *4*, 345−392.

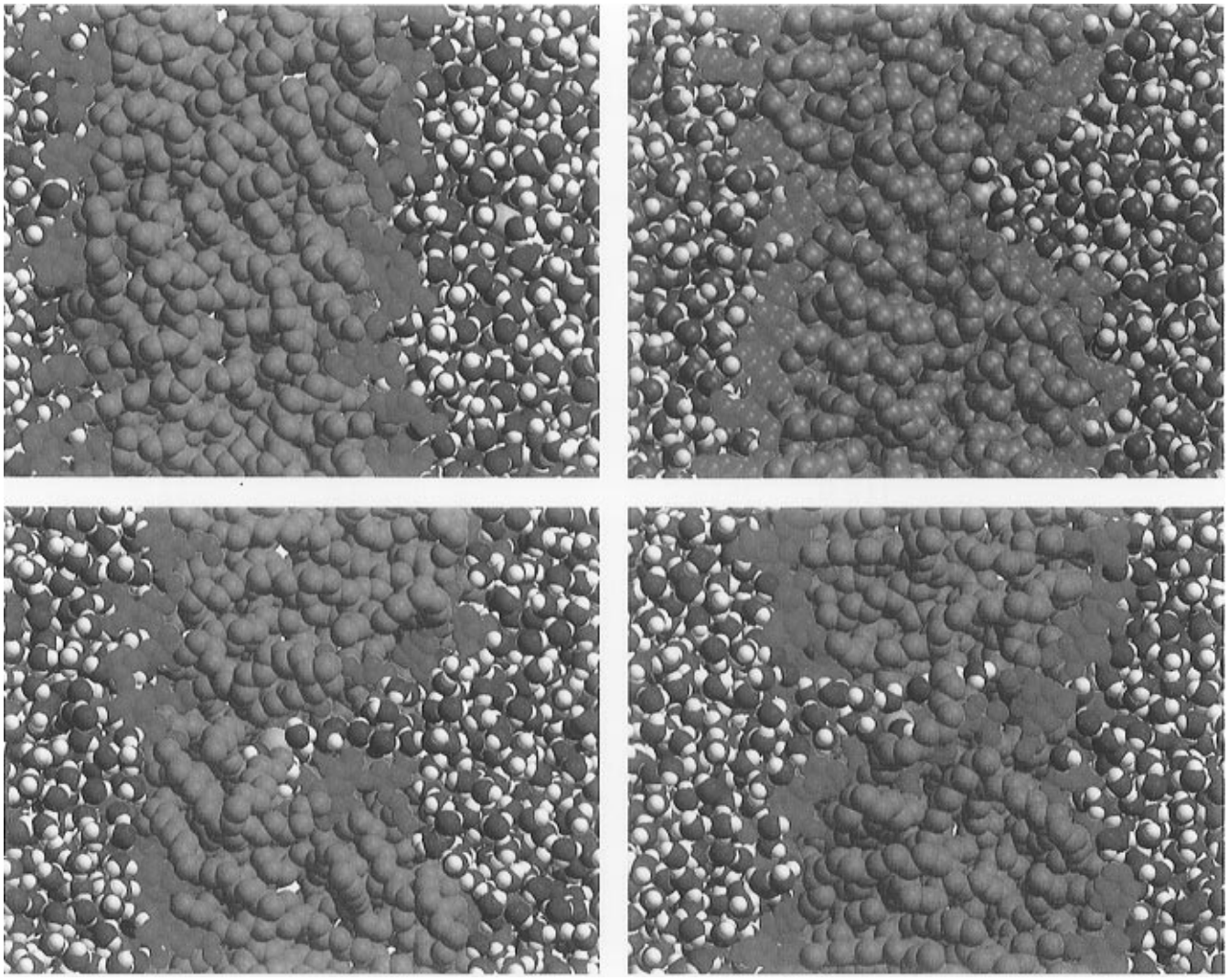

Figure 1. Four representative configurations of Na^+ in the water−GMO system obtained from molecular dynamics simulations (a) as the ion approaches the membrane from the water (upper left), (b) as the ion penetrates the head group region of the membrane (upper right), (c) as the ion crosses the midplane of the membrane (lower left), and (d) as the ion moves through the outgoing side of the membrane (lower right). The ion is yellow, the GMO tails are blue, the GMO head groups are magenta, and the oxygen and hydrogen atoms of water molecules are red and white, respectively.

the system. The direct application of this method would not yield accurate results because the free energy changes steeply even within a relatively narrow range, *e.g.*, 5 Å. Consequently, this range would be sampled with considerably nonuniform probability. To improve the statistical precision, the umbrella sampling method[26] was used, whereby a biasing function $U_b(z)$ was added which yielded a more uniform sampling of z. Then, $\Delta A(z)$ was related to the biased probability distribution, $P_b(z)$, within the range by the formula

$$\Delta A(z) = -kT\ln P_b(z) + U_b(z) \qquad (3)$$

In practice, a linear biasing potential of the form $U_b(z) = Bz$ was used. Since consecutive ranges of z overlapped, the full free energy profile was constructed by requiring that $A(z)$ be a continuous function of z. This was done by the weighted histogram analysis method.[27]

The ranges of each window along z, the lengths of trajectories in these windows, and the corresponding biasing potentials $U_b(z)$ are listed in Table 1. The ion was restrained within a window by a cubic potential $k(z_{min} - z)^3$ for $z < z_{min}$ and $k(z - z_{max})^3$ for $z > z_{max}$, where z_{min}, z_{max} are the lower and upper bounds of the window. The center of mass of the system was kept at $z = 0$. Calculations in each window were carried out until the statistical error (± one standard deviation) for $A(z_{max}) - A(z_{min})$, obtained by treating $A(z)$ from 10 ps segments of the trajectory as independent measurements, was smaller than 0.5 kcal/mol.

III. Results and Discussion

Molecular Mechanism of Ion Transport. A clear illustration of the mechanism by which Na^+ is transported across the bilayer is provided in Figure 1. The ion located in water has no influence on the structure of the bilayer (Figure 1a). When it enters and moves through the head group region of the membrane, it remains solvated not only by water molecules but also by GMO head groups. This creates a disruption on the incoming side of the membrane whereby the polar head groups follow the ion and "cave in" forming a "bay" filled with water molecules (Figure 1b). With further translocation of the ion

(26) (a) Bennett, C. H. In *Algorithms for Chemical Computations: ACS Symposium Series 46*; Christofferson, R. E., Ed., American Chemical Society: Washington, D.C., 1977. (b) Valleau, J. P.; Torrie, G. M. In *Statistical Mechanics A. Modern Theoretical Chemistry*; Berne, B. J., Ed., Plenum Press: New York, Vol. 5, pp 169−194.

(27) Kumar, S.; Bouzida, D.; Swendsen, R. H.; Kollman, P. A.; Rosenberg, J. M. *J. Comput. Chem.* **1992**, *13*, 1011−1021.

Table 1. Trajectory Information from the Calculation of Na^+ and Cl^- in the Water−GMO Bilayer System

Na^+				Cl^-			
z_{min}	z_{max}	t (ps)	*B* (kcal/mol-Å)	z_{min}	z_{max}	t (ps)	*B* (kcal/mol-Å)
−26	−20	610	0.0	−35	−25	1000	0.0
−21	−15	650	−1.5	−26	−20	950	0.0
−16	−10	280	−3.0	−21	−16	980	−1.2
−11	−5	500	−2.0	−18	−13	1000	−1.2
−6	−1	1000	−2.0	−14	−9	1500	−2.5
−3	3	2000	0.0	−10	−5	500	−4.0
1	6	500	2.0	−7	−1	1000	−2.0
5	−10	850	6.0	−3	3	1500	0.0
9	14	1000	2.5	1	7	600	2.0
13	18	600	2.5	6	12	800	1.0
16	21	980	1.2	11	17	600	1.0
20	26	900	0.0	16	22	1600	1.0
25	35	900	0.0	21	27	800	0.0

toward the middle of the membrane the defect in this side of the bilayer deepens (Figure 1c). As the ion crosses the midplane of the bilayer the deformation "switches sides"; the initial defect slowly relaxes, and a defect forms in the outgoing side of the bilayer (Figure 1d).

In the observed mechanism, the ion does not undergo extensive desolvation. For Na^+, the calculated hydration number (the average number of water molecules in the first hydration shell around the ion), N_h, in bulk water is 5.4. As summarized in Table 2, N_h is reduced as the ion is transferred into the membrane and reaches approximately 3.5 near the center. As the hydration of the ion decreases, its solvation by the oxygen atoms of the GMO head groups increases. This solvation number, N_s, which is the average number of oxygen atoms of GMO molecules around the ion, is in the range 0.8−2.5 inside the bilayer. While both N_h and N_s vary, the total solvation number ($N_{tot} = N_h + N_s$) is remarkably constant at 5.5 ± 0.3 throughout the transfer process. Even in the middle of the bilayer, where N_h and N_s fluctuate markedly, N_{tot} remains unchanged.

The large fluctuations in the structure of the solvation shell near the transition state reflect the changes accompanying ion transfer through the middle of the bilayer. As the head groups on the incoming side of the bilayer start to relax, the ion attracts an additional water molecule to compensate for the loss of GMO oxygen atoms in its first solvation shell. Subsequent formation of a defect on the outgoing side leads again to the increase in ion solvation by oxygen atoms of the head groups. The additional water molecule is then removed from the first solvation shell around the ion.

The transport of Cl^- proceeds by a similar mechanism as the transport of Na^+, *i.e.*, it is also accompanied by the formation of membrane defects. There are, however, differences in the patterns of solvation around these two ions. Na^+ interacts primarily with negatively charged oxygen atoms of the water and GMO head groups. In particular, about half of the head group atoms solvating Na^+ in the center of the bilayer are carbonyl oxygens. In contrast, these atoms do not contribute to the first solvation shell around Cl^- which consists entirely of hydroxyl groups from water and GMO molecules. These groups are oriented such that positively charged hydrogen atoms point toward the ion. Furthermore, one of the seven OH groups in the first solvation shell around Cl^- in water is lost in the interior of the bilayer.

Further information about ion hydration is provided by the radial distribution function of oxygen atoms of water around Na^+, shown in Figure 2. As the ion moves into the membrane, the first and second peaks in the radial distribution function

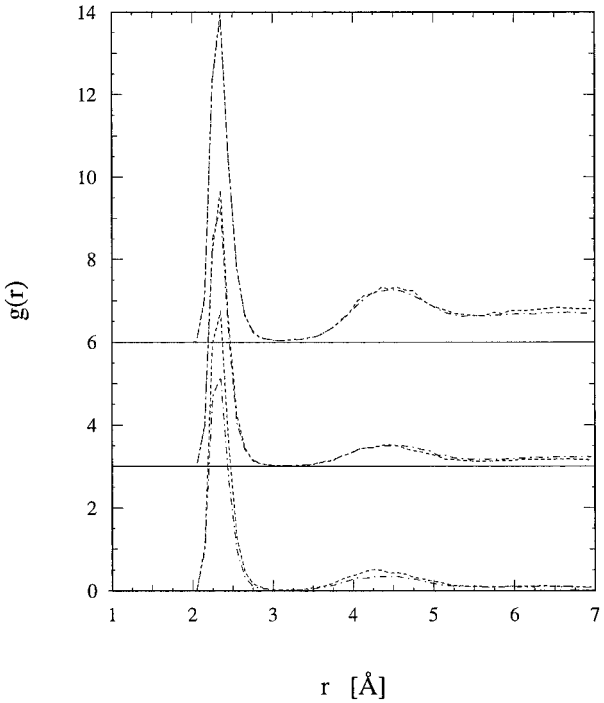

Figure 2. Na^+−water oxygen radial distribution function, g(r) when the ion is 17 Å (upper), 8 Å (middle), and 3 Å (lower) from the midplane of the bilayer either on the incoming side (dotted line) or on the outgoing side (dot-dashed line).

are reduced but remain in the same location. Similarly, the first minimum in the membrane is identical to the first minimum in water. However, the radial distribution function does not reach zero at any distance beyond the second peak, even when the ion is in the middle of the bilayer. This indicates that water molecules surrounding the ion remain "connected" to the bulk water, and the ion should not be considered as a hydrated charge embedded in the membrane.

The ability of ions to remain well solvated near aqueous interfaces has already been noted in computer simulations of Na^+, Cl^-, and F^- at the water liquid−vapor interface.[28] Furthermore, a recent molecular dynamics study revealed that the transfer of Cl^- from 1,2-dichloroethane to water is preceded by the formation of water "fingers" (chains of water molecules connecting the ion with the aqueous phase).[29] These water fingers facilitate transfer of the ion from the organic phase to water. Such a mechanism is similar to the formation of a water-filled defect in the membrane, spanning the region between the ion and the water surface. In particular, creation of such defects in the outgoing side of the membrane is required for successful ion transfer, preventing it from returning to the incoming water lamella.

Free Energy Barriers. Our simulations not only provide a molecular-level description of unassisted ion transport but also allow for estimating the free energy profiles of the ions. These profiles are shown in Figure 3. Previously, the free energy changes across water-membrane systems were obtained from molecular dynamics simulations for several small, uncharged solutes.[30−33] The calculated free energy barrier for Na^+ is equal to 54 kcal/mol and is located in the middle of the membrane.

(28) (a) Wilson, M. A.; Pohorille, A. *J. Chem. Phys.* **1991**, *95*, 6005−6013. (b) Benjamin, I. *J. Chem. Phys.* **1991**, *95*, 3698−3709.
(29) Benjamin, I. *Science* **1993**, *261*, 1558−1560.
(30) Bassolino-Klimas, D.; Alper, H. E.; Stouch, T. R. *J. Am. Chem. Soc.* **1995**, *117*, 4118−4129.
(31) (a) Xiang, TX.; Anderson, B. D. *J. Membr. Biol.* **1994**, *140*, 111−122. (b) Xiang, TX.; Anderson, B. D. *J. Membr. Biol.* **1995**, *148*, 157−167.

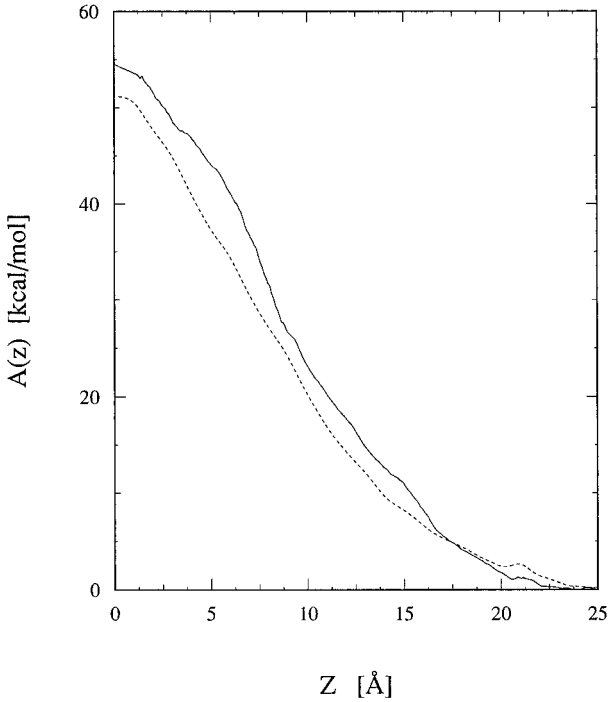

Figure 3. The free energy profile of transferring Na^+ (solid line) and Cl^- (dashed line) from water to the center of the GMO bilayer. $z = 0$ corresponds to the middle of the membrane, and the membrane−water interface is located approximately at 18 Å.

The barrier for Cl^- is 3.5 kcal/mol lower. The free energy profiles are slightly asymmetric with respect to the middle of the bilayer. This is in part due to terminating the simulations before the bilayer fully relaxed on the outgoing side. However, difficulties in determining accurately the free energy profile inside the bilayer undoubtedly also contribute to the observed asymmetry.

Since the united atoms of the GMO tails do not carry partial charges and are not polarizable, ϵ_b of the membrane interior in this model is equal to 1 rather than 2, as expected for real membranes. Thus, the free energy barrier obtained from our molecular-level simulations that allow for membrane deformations should be compared to predictions of the dielectric model at $\epsilon_b = 1$. For Na^+, $\Delta A(TS)$ from computer simulations is equal to approximately 60% of $\Delta A(TS)$ from the dielectric model. When the dielectric constant of the membrane interior is increased to 2, $\Delta A(TS)$ from the model is reduced to 52% of its value at $\epsilon_b = 1$. If the same scaling is applied to the results obtained from computer simulations (assuming that a slight polarizability of the bilayer interior does not significantly change the mechanism of transport), the actual barrier encountered by Na^+ can be estimated at 27 kcal/mol.

To test whether the scaling factor, $\Delta A(TS)_{\epsilon_b=1}/\Delta A(TS)_{\epsilon_b=2}$, appropriate for the "naked" ion inside the membrane, also applies to a partially solvated ion, a series of continuum dielectric model calculations was performed. In these calculations, the Poisson equation for the ion with nearby water molecules and GMO headgroups in media of dielectric constants 1 and 2 was solved using the boundary elements method.[34] Five such clusters were generated from five randomly selected configurations from the molecular dynamics simulations in which the ion was located near the center of the bilayer. Each cluster consisted of all water molecules and GMO headgroups that had at least one atom within 3.5 Å from the ion. Thus, 31 or 37 atoms (three water molecules and two headgroups or two water molecules and three head groups) were retained in the cluster. Each atom carried a discrete charge equal to the charge used in the molecular dynamics simulations. From the continuum dielectric calculations we obtained the free energies of the ion in each cluster (relative to vacuum). The knowledge of these free energies allowed us to calculate the ratio $\Delta A(TS)_{\epsilon_b=1}/\Delta A(TS)_{\epsilon_b=2}$. For the five clusters, its value remained in a narrow range between 0.52 and 0.56, very close to the value obtained for the unsolvated ion, thus supporting our estimate of the free energy barrier.

A further approximation involved in our calculations regards the neglect of long-range effects. Recently several methods have been developed to include efficiently these effects.[35] However, it is not clear whether they are applicable to our system. An interesting perspective on the magnitude of long-range effects can be gained by observing that even when the ion is near the midplane of the bilayer it experiences long-range interactions mostly from water molecules. This is reflected in the second (logarithmic) term in eq 1. For example, the contributions to $\Delta A(TS)$ from interactions between Na^+ and the medium beyond 12 Å, calculated from this equation, is 6.1 and 2.9 kcal/mol for $\epsilon_b = 1$ and $\epsilon_b = 2$, respectively. Similar contributions to the free energy of transfer from water to a nonpolar medium are more than twice as large, 13.7 and 6.7 kcal/mol. In addition, we note that, in contrast to phospholipids, GMO headgroups do not contain atoms with large partial charges that could markedly contribute to long-range effects.

Estimates of the Permeability Coefficient. The permeability coefficient, P, of the membrane to Na^+ can be calculated under standard assumptions[36,37] from the diffusion model[33]

$$P = 1/\int_{z_1}^{z_2} \frac{e^{\beta\Delta A(z)}}{D(z)} dz \qquad (4)$$

where D is the diffusion coefficient of the ion, dependent in general on z, $\beta = 1/kT$, and the limits of integrations are positions in water on both sides of the bilayer.

In the high barrier limit, $\Delta A(z)$ can be expanded around the free energy in the transition state $\Delta A(TS)$ located at z_{TS} (the mid-plane of the bilayer)

$$\Delta A(z) = \Delta A(TS) + \frac{1}{2}\frac{\partial^2 \Delta A}{\partial z^2}\Big|_{z_{TS}} (z - z_{TS})^2 \qquad (5)$$

It can be further assumed that the diffusion coefficient is constant in the interior of the bilayer, near the transition state, and is equal to D_b. Then we obtain

$$P = D_b e^{-\beta\Delta A(TS)} / \int_{z_1}^{z_2} e^{-\beta a (z - z_{TS})^2} dz \qquad (6)$$

where $a = {}^1/_2 |\partial^2 \Delta A/\partial z^2|_{z_{TS}}|$. Without appreciable loss of accuracy we can substitute the limits of integration in the

(32) (a) Pohorille, A.; Wilson, M. A. *J. Chem. Phys.* **1996**, *104*, 3760−3773. (b) Pohorille, A.; Cieplak, P.; Wilson, M. A. *Chem. Phys.* **1996**, *204*, 337−345.

(33) Marrink, S.-J.; Berendsen, H. J. C. *J. Phys. Chem.* **1994**, *98*, 4155−4168.

(34) Pratt, L. R. unpublished results. The method used is described: Tawa, G. J.; Pratt, L. R. Structure and Reactivity in Aqueous Solution, Characterization of Chemical and Biological Systems; ACS Symposium Series 568; Cramer, C. J., Truhlar, D. G., Eds.; 1994; pp 60−70.

(35) (a) Darden, T.; York, D.; Pedersen, L. *J. Chem. Phys.* **1993**, *99*, 10089−10092. (b) White, C. A.; Head-Gordon, M. *J. Chem. Phys.* **1994**, *101*, 6593−6605. (c) Procacci, P.; Marchi, M. *J. Chem. Phys.* **1996**, *104*, 3003−3012.

(36) Schulten, K.; Schulten, Z.; Szabo, A. *J. Chem. Phys.* **1981**, *74*, 4426−4432.

(37) Cooper, K. E.; Gates, P. Y.; Eisenberg, R. S. *J. Membrane Biol.* **1988**, *106*, 95−105.

gaussian integral in eq 6 by $[-\infty,\infty]$. Then we obtain

$$P = \sqrt{\frac{\beta a}{\pi}} D_b e^{-\beta \Delta A(TS)} \tag{7}$$

Comparing eqs 4 and 7 we note that in the high barrier limit the diffusion coefficient needs be known only in the vicinity of the transition state. This is a good approximation for simple ions permeating membranes but not necessarily for uncharged solutes. D_b was estimated at 10^{-4} cm s^{-1}. This corresponds to an increase in the diffusion coefficient in the membrane interior over that in water by a factor of 7.[38] A similar value of D was calculated for water, a molecule with the same mass as Na^+, diffusing in the interior of the bilayer.[33] Then, P calculated from eq 4 is equal to 0.3×10^{-15} cm s^{-1}. A similar value is obtained by applying a simplified eq 7.

Alternatively, P can be calculated from the transition state theory.[39] Then, P is expressed as

$$P = \sqrt{\frac{kT}{m}} e^{-\beta \Delta A(TS)} \tag{8}$$

Here m is the mass of the ion. For $\Delta A(TS)$ estimated above, $P = 0.8 \times 10^{-15}$ cm s^{-1}.[40]

There has been some controversy as to which of these two methods is appropriate for calculating rates of transporting ions across membranes, especially through ion channels.[37] Here, as we can see, both methods yield similar results, in the range of $10^{-15}-10^{-16}$ cm s^{-1}, because the Kramers' limit of high barrier applies in this case. The permeability of the GMO bilayer to ions is not known, but, by comparison, the measured permeabilities of different phospholipid bilayers to Na^+ are of the order of $10^{-12}-10^{-15}$ cm s^{-1} [3,5,8], in qualitative agreement with our estimate.

Applying the same arguments as before, we obtain the membrane permeability to Cl^- approximately 1−2 orders of magnitude higher than the permeability to Na^+. A similar result was observed experimentally.[3]

The uncertainty in $\Delta A(TS)$ estimated from the statistical errors within the individual ranges along z is approximately 3 kcal/mol. A slightly higher uncertainty is obtained from the overall asymmetry of the free energy profiles (*i.e.*, the free energy difference of transferring the ion between water lamellae on the incoming and outgoing sides of the bilayer). This corresponds to an uncertainty in P of 2−3 orders of magnitude.

Discussion of the Mechanism of Ion Transport. To explain why the formation of thinning defects is the most likely mechanism of ion transfer we appeal to our understanding of membrane fluctuations in the pure water−bilayer system. We have previously shown that surfaces of the GMO bilayer are quite flexible and fluctuate according to the capillary wave model.[20] Surface fluctuations were also observed in both experiments[41,42] and computer simulations[30,43] on phospholipid bilayers and surfactants. Fluctuations of both surfaces of GMO bilayers are independent, yielding a Gaussian distribution of instantaneous widths of the bilayer. These results show that thinning defects form spontaneously in the membrane on a time scale of computer simulations (several nanoseconds). Equivalently, the unfavorable free energy associated with the formation of an asymmetric defect is only modest. In the presence of an ion, such defects are even more probable. However, the formation of symmetric defects on both sides of the bilayer (pores) appears to be too disruptive. For pure membranes, these events are unlikely because they require *simultaneous* deformations of independently fluctuating membrane surfaces. In the presence of the ion, the free energy cost of perturbing both sides of the bilayer is not compensated by the gain in the free energy of solvating the ion since the ion is able to retain its first solvation shell even in the case of asymmetric defects.

Since the probability of forming spontaneous thinning defects in the bilayer decreases exponentially with their depth,[20] it can be anticipated that the ionic permeabilities of thin membranes depend on the length of the hydrocarbon tails more strongly than predicted by the dielectric model. This prediction appears to be confirmed by measurements of efflux of K^+ from liposomes built of phosphatidylcholines with tails containing 14, 16, and 18 carbon atoms.[8]

One can raise a question if other mechanisms of transferring an ion from water to the middle of the bilayer are probable. This was tested by placing a fully desolvated Na^+ in the center of the unperturbed membrane and keeping the ion constrained to the midplane of the bilayer. Responding to the presence of the ion, the membrane slowly developed a defect located mostly on one side of the bilayer. As can be seen from the change in the ion solvation numbers (Table 3), initial movement of GMO head groups to solvate the ion was followed by penetration of water molecules into the developing defect. After 1 ns, both N_h and N_s reached values close to those observed around the ion at the same location during the transfer process (see Table 2). Note that the structure of the defect, shown in Figure 4, is remarkably similar to the defects shown in Figure 1 (lower left and right). These similarities, combined with the fact that the time scale of forming the defect is shorter than the time scale of the free energy calculations described previously, give us some confidence that both the mechanism and the free energy profiles of ion transport presented here are qualitatively correct.

A possibility of forming stable, symmetric defects in the membrane was tested in a computer simulation in which two particles carrying a charge of 0.5 e were simultaneously moved from both sides of the bilayer to the middle. Initially, this movement was accompanied by the formation of defects in each side of the membrane. However, when both particles reached the middle and coalesced to Na^+, one of the defects relaxed yielding, again, an asymmetric membrane deformation. These simulations demonstrate that pores in the bilayer are not stable structures during ion transport.

(38) A similar increase was obtained in computer simulations of ion transfer across the interface between a polar and a nonpolar liquid (Benjamin, I. *J. Chem. Phys.* **1992**, *96*, 577−585) and is close to the ratio of dielectric friction to viscous drag for Na^+ in water predicted by the Zwanzig's theory (Berkowitz, M.; Wan, W. *J. Chem. Phys.* **1987**, *86*, 376−382). The position-dependent diffusion constant can also be calculated in molecular dynamics simulations, as described in ref 33. However, for a united atom model of hydrocarbon chains this is not likely to be more accurate than the estimate discussed here.

(39) (a) Chandler, D. *J. Chem. Phys.* **1978**, *68*, 2959−2970. (b) Berne, B. J.; Borkovec, M.; Straub, J. E. *J. Phys. Chem.* **1988**, *92*, 3711−3725.

(40) Since, contrary to the assumptions of the transition state theory, not all trajectories of the ion initiated on one side of the bilayer reach the opposite side, P should be multiplied by the transmission coefficient, κ, that corrects for this fact. In the simplest model, (a) the trajectory is reactive (leads to a successful ion transfer) only if it is accompanied by a fluctuation defect on the outgoing side of the membrane, and (b) the probabilities of finding a defect on either side of the membrane are identical. Then $\kappa = 0.5$.

(41) (a) Wiener, M. C.; King, G. I.; White, S. H. *Biophys. J.* **1992**, *60*, 568−576. (b) Wiener, M. C.; White, S. H. *Biophys. J.* **1992**, *61*, 434−447.

(42) Lu, J. R.; Hromadova, M.; Thomas, R. K. *Langmuir* **1993**, *9*, 2417−2425.

(43) (a) Egberts, E.; Berendsen, H. J. C. *J. Phys. Chem.* **1988**, *89*, 3718−3732. (b) Damodaran, K. V.; Merz, K. M.; Garber, B. P. *Biochemistry* **1992**, *31*, 7656−7664. (c) Raghavan, K.; Reddy, M. R.; Berkowitz, M. L. *Langmuir* **1992**, *8*, 233−240.

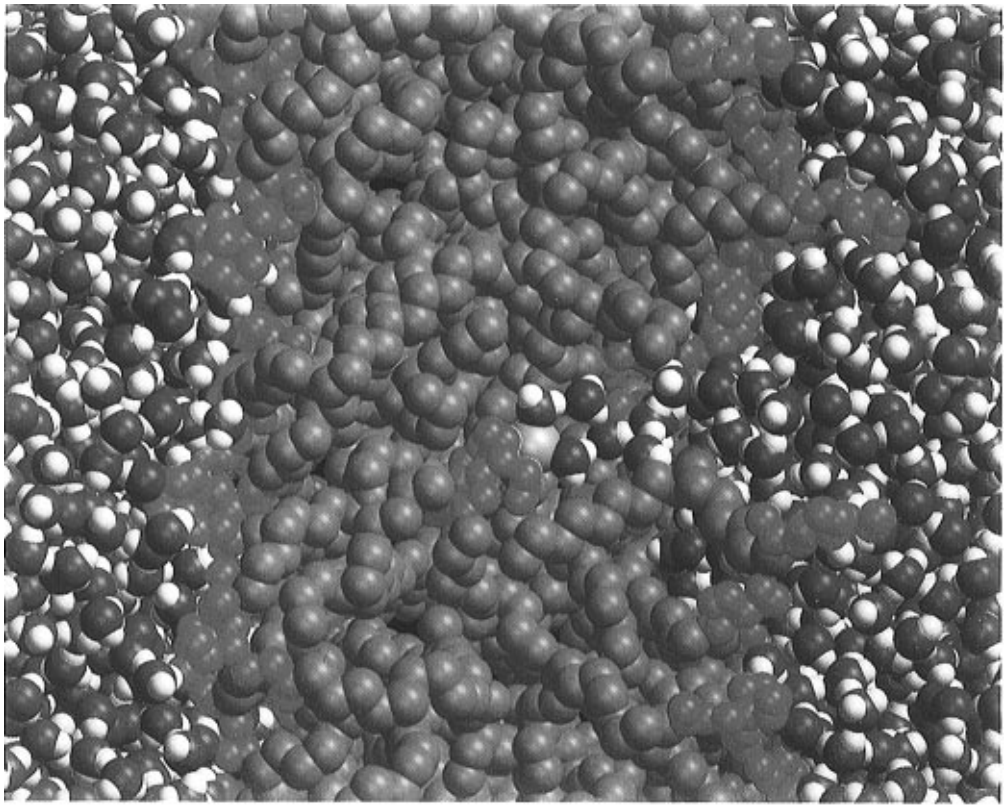

Figure 4. A representative configuration of the water−GMO system 1 ns after placing Na^+ in the middle of the unperturbed bilayer. Color coding is the same as in Figure 1.

Table 2. Hydration Number, N_h, GMO Oxygen Solvation Number, N_s, and the Total Solvation Number, N_{tot}, of Na^+ as a Function of Its Position in the Bilayer

range (Å)[a]	N_s^b	N_h^b	N_{tot}
18.5	0.2	5.2	5.4
15.5	0.4	5.0	5.4
11.5	1.5	4.1	5.6
7.5	1.4	4.1	5.5
3.5	2.3	3.3	5.6
0[c]	2.1	3.5	5.6
0[c]	1.4	3.8	5.2
0[c]	0.8	4.5	5.3
−3.5	2.5	3.3	5.8
−8.0	1.3	4.2	5.5
−13.0	0.6	4.9	5.5
−18.0	0.2	5.3	5.5
−23.0	0.0	5.4	5.4

[a] $z = 0$ at the center-of-mass of the system (which approximately corresponds to the middle of the bilayer). The positions correspond to the centers of bins 5 or 6 Å wide. Membrane−water interfaces are located at ±18 Å. [b] The average number of oxygen atoms within the radius of 3.15 Å from Na^+. This radius corresponds to the first minimum in the Na^+−water oxygen radial distribution function. [c] Results for three consecutive 200 ps fragments of the molecular dynamics trajectory.

Finally, we discuss the likelihood that the transition state consists of an ion with its tightly bound first hydration shell located in the middle of the otherwise unperturbed membrane. Previous estimates of the energetics of this state yielded $\Delta A(TS)$ in apparent agreement with experimental values.[3,8] However, the free energy cost of removing the water molecules around the ion from the aqueous medium was incorrectly neglected in these estimates. Once this contribution is included, $\Delta A(TS)$ increases markedly, and no longer agrees with the experimental results. This can be seen by considering $\Delta A(TS)$ for Na^+ as a sum of contributions from (1) transferring the ion from water to the gas phase ($\Delta A_i^{w\rightarrow g}$), (2) removing five water molecules from water to the gas phase such that they do not interact among themselves ($\Delta A_{5w}^{w\rightarrow g}$), (3) forming a cluster of Na^+ and five water molecules in the gas phase (ΔA_c^g), and (4) placing the cluster in the interior of the bilayer ($\Delta A_c^{g\rightarrow b}$). The first three contributions are known from experiments: $\Delta A_i^{w\rightarrow g} = 98.5$ kcal/mol,[44] $\Delta A_{5w}^{w\rightarrow g} = 5 \times 6.3 = 31.5$ kcal/mol,[45] and $\Delta A_c^g = -50.3$ kcal/mol.[46] The only quantity that remains to be estimated is $\Delta A_c^{g\rightarrow b}$. Its electrostatic part was calculated by solving the Poisson equation for the cluster in a medium of dielectric constant equal to 2 and was found to be −38.6 kcal/mol.[47] By summing up these contributions, we obtain an estimate of $\Delta A(TS)$ of 41 kcal/mol. This value has to be corrected for the finite width of the membrane and the nonelectrostatic part of $\Delta A_c^{g\rightarrow b}$, consisting of an unfavorable

Table 3. Hydration Number, N_h, GMO Oxygen Solvation Number, N_s, and the Total Solvation Number, N_{tot}, of Na^+ Restricted to the Midplane of the Bilayer as a Function of Time[a]

time (ps)	N_s	N_h	N_{tot}
100−200	0.0	0.0	0.0
300−400	2.3	0.0	2.3
400−500	4.1	0.0	4.1
500−600	4.8	0.6	5.4
600−700	4.0	1.8	5.8
700−800	4.0	1.8	5.8
800−900	3.9	1.7	5.6
900−1000	2.3	3.0	5.3

[a] The ion was placed in the unperturbed membrane at time $t = 0$. N_h and N_s are defined as in Table 2.

(44) Burgess, M. A. *Metal Ions in Solution*; Ellis Harwood: Chichester, England, 1978.
(45) Ben Naim, A.; Marcus, Y. *J. Chem. Phys.* **1984**, *81*, 2016−2027.
(46) Džidić, I.; Kaberle, P. *J. Phys. Chem.* **1970**, *74*, 1466−1474.
(47) Tawa, G. J.; L. R. Pratt, unpublished results. For description of the method used see ref 34. For the geometry of the system used to calculate $\Delta A(TS)$ in eq 1, the electrostatic energy is expected to be approximately 2 kcal/mol lower.

free energy needed to create a cavity in the membrane that can accommodate the cluster and a favorable cluster-membrane van der Waals energy. These corrections, however, are small[48] and will not bring the calculated and experimental values of $\Delta A(TS)$ into agreement. Thus, a transition state for ion transport that involves a hydrated ion embedded in the membrane interior is inconsistent with the observed permeabilities of membranes to ionic species.

IV. Conclusions

In summary, the flexibility of the bilayer yields the mechanism of unassisted ion transport across asymmetric thinning defects in the membrane. In this mechanism, the GMO head groups on the incoming side of the bilayer follow the movement of the ion into the membrane interior by tilting inwards. The resulting defect is filled with water. Once the ion crosses the midplane of the bilayer, the defect on the incoming side of the membrane disappears and, instead, a similar deformation is formed on the outgoing side. During the transfer, the ion remains solvated by GMO head groups and water molecules. Even though the calculated ionic permeabilities are subject to considerable uncertainties, we showed that this mechanism qualitatively accounts for a large increase in these permeabilities (by 14−17 orders of magnitude), compared to the estimates from the rigid membrane model. In contrast, alternative mechanisms involving formation of pores in the membrane or the existence of an ion−water cluster in the nonpolar interior of the bilayer are not supported by the calculations and are inconsistent with our understanding of membrane structure and the energetics of unassisted ion transport.

In agreement with experimental data,[8] our results imply that the permeability of thin membranes to ions should change with the bilayer width more rapidly than expected from the continuum dielectric model. This offers, for example, a possibility of regulating release of charged therapeutic agents from liposomes.

The calculations also illustrate the broader point that polar groups and/or molecules in the membrane can readily reorganize to stabilize a charge inside the bilayer. It is likely that this effect should be considered, for example, in the studies of the mechanism by which peptides are incorporated into lipid bilayers.

With growing computational resources, several extensions of this work can be envisioned. Probably the most interesting would be to investigate ionic permeability as a function of hydrocarbon chain length in phospholipid bilayer. Methodologically, the most important extension would be to use an all-atom model of hydrocarbon chains in which both carbon and hydrogen atoms would carry small partial charges such that the dielectric constant in the membrane interior would be correctly reproduced. We are pursuing both these extensions.

Acknowledgment. This work was supported by a grant from the NASA Exobiology Program (UCSF−NASA Ames Cooperative Agreement NCC 2-772). Computer facilities were provided by the NASA Aerodynamic Simulator (NAS) and by the Supercomputer Center at the National Cancer Institute. The authors thank Dr. Lawrence Pratt and Dr. G. Tawa for calculating the electrostatic free energy of the solvated Na^+ in a medium of the dielectric constant equal to 2.

JA9540381

(48) The free energy of forming in hexane a cavity of the 4.2 Å radius, which corresponds to the size of the cluster, estimated by extrapolating the data: Pohorille, A.; Pratt, L. R. *J. Am. Chem. Soc.* **1990**, *112*, 5066−5074 is 16 kcal/mol. Inside the bilayer, this value is expected to be somewhat lower due to a lower density of alkyl groups in the hydrocarbon core of the membrane. The van der Waals energy of interactions between the cluster and 256 hexane molecules obtained from 50 ps of molecular dynamics simulations is −10 kcal/mol. An estimate of the correction for the width of the membrane from the dielectric model (eq 1) is −3.7 kcal/mol.